The importance of laboratory water quality for studying initial bacterial adhesion during NF filtration processes

A.J.C. Semião [§], O. Habimana [§], H. Cao, R. Heffernan, A. Safari, E. Casey [*]

School of Chemical and Bioprocess Engineering, University College Dublin (UCD), Belfield, Dublin 4, IRELAND

[§]Both authors contributed equally to this work

*Corresponding author. Mailing address: University College Dublin, School of Chemical and Bioprocess Engineering, Belfield, Dublin 4, IRELAND. Phone: +353 1 716 1974. Email: eoin.casey@ucd.ie

Keywords: Compaction, water quality, cell adhesion, nanofiltration

Abstract

Biofouling of nanofiltration (NF) and reverse osmosis (RO) membranes for water treatment has been the subject of increased research effort in recent years. A prerequisite for undertaking fundamental experimental investigation on NF and RO processes is a procedure called compaction. This involves an initial phase of clean water permeation at high pressures until a stable permeate flux is reached. However water quality used during the compaction process may vary from one laboratory to another. The aim of this study was to investigate the impact of laboratory water quality during compaction of NF membranes. A second objective was to investigate if the water quality used during compaction influences initial bacterial adhesion.

Experiments were undertaken with NF270 membranes at 15 bar for permeate volumes of 0.5L, 2L, and 5L using MilliQ, deionized or tap water. Membrane autopsies were performed at each permeation point for membrane surface characterisation by contact angle measurements, profilometry, and scanning electron microscopy. The biological content of compacted membranes was assessed by direct epi-fluorescence observation following nucleic acid staining. The compacted membranes were also employed as substrata for monitoring the initial adhesion of *Ps. fluorescens* under dynamic flow conditions for 30 minutes at 5 minutes intervals.

Compared to MilliQ water, membrane compaction using deionized and tap water led to decreases in permeate flux, increase in surface hydrophobicity and led to significant build-up of a homogenous fouling layer composed of both living and dead organisms (>10^6

cells.cm^{-2}). Subsequent measurements of bacterial adhesion resulted in cell loadings of 0.2×10^5, 1.0×10^5 cells×cm^{-2} and 2.6×10^5 cells.cm^{-2} for deionized, tap water and MilliQ water, respectively. These differences in initial cell adhesion rates demonstrate that choice of laboratory water can significantly impact the results of bacterial adhesion on NF membranes. Standardized protocols are therefore needed for the fundamental studies of bacterial adhesion and biofouling formation on NF and RO membrane. This can be implemented by first employing pure water during all membrane compaction procedures and for the modelled feed solutions used in the experiment.

1 Introduction

Nanofiltration (NF) and reverse osmosis (RO) membranes are commonly used for the removal of organic matter and trace contaminants, such as pesticides, during water treatment processes (Cyna et al. 2002). The efficiency of NF and RO processes is however adversely affected by membrane biofouling (Flemming 1997, Ivnitsky et al. 2007), principally due to the formation of biofilms (Flemming 2002). These ecosystems are usually made up of a community of dead and living microorganisms held together by a matrix of polysaccharides, lipids, proteins, organic matter, amongst other components (Flemming 2002). Biofilms are ubiquitous in NF and RO membrane plants (Houari et al. 2009, Vrouwenvelder et al. 1998, Vrouwenvelder et al. 2008, Khan et al. 2013) and are the Achilles heel of NF and RO processes (Flemming et al. 1997) as they are difficult to remove (Hijnen et al. 2012). Biofouling increases pressure drop along the membrane module (Vrouwenvelder et al. 2009a, Hijnen et al. 2009), leading to increased costs associated with energy consumption. The presence of biofilms on the membrane surface has also been shown to significantly affect permeate flux, and solute retention (Ivnitsky et al. 2005, Huertas et al. 2008). The decrease in solute retention and permeate flux has been attributed to enhanced concentration polarisation caused by the biofilms (Herzberg and Elimelech 2007). It has been shown that the concentration polarization also maintains the presence of biofilms by concentrating nutrients from the bulk environment (Chong et al. 2008, Vrouwenvelder et al. 2009b).

Biofilm formation is initiated by the irreversible adhesion of bacterial cells onto the membrane's surface, which is influenced by a number of factors. Firstly, the cell properties

such as hydrophobicity (Ridgway et al. 1985) and cell surface charge (Subramani and Hoek 2008) have been found to affect adhesion. Secondly, the membrane physicochemical properties (roughness, charge and hydrophobicity) have been shown to impact the degree of adhesion. In general, the rougher and the more hydrophobic the membrane is, the more cells will adhere to the surface (Subramani and Hoek 2008, Myint et al. 2010, Khan et al. 2011). Finally, the presence of a conditioning layer on the membrane also affects bacterial adhesion (Subramani et al. 2009). A recent study has shown that a conditioning layer of salts and organic carbon promoted a homogeneous biofilm, whilst the absence of a conditioning layer resulted in a scattered and thin biofilm (Baek et al. 2011).

The intractable nature of the biofouling problem has led to a significant increase in research in this area in recent years (Herzberg and Elimelech 2007, Chong et al. 2008, Subramani and Hoek 2008, Baek et al. 2011, Fonseca et al. 2007). These studies range from the effects of biofilms on process performance (Ivnitsky et al. 2005, Huertas et al. 2008) to biofouling control through the design of antifouling membranes (Miller et al. 2012, Bernstein et al. 2011). Although membrane biofouling research methodologies differ from one research laboratory to another, they generally share a common pre-treatment procedure involving the compaction of the studied membrane prior to biofouling experiments. To accurately monitor flux changes and solute retention during NF and RO experiments caused by osmotic pressure or membrane fouling, membranes are purposely compacted to prevent changes due to the effect of pressure during the experiment. The compaction of NF and RO membranes is carried out under different filtration conditions depending on the laboratory they are carried out. The compaction is typically undertaken at a pressure between 6 and 25 bar and up to 18 hours in duration (Herzberg and Elimelech 2007, Baek et al. 2011, Fonseca

et al. 2007, Suwarno et al. 2012). This translates into a typical water permeation volume between 2 L (membrane flux=50 $L.h^{-1}.m^{-2}$, time=18 hours and 22.44 cm^2 membrane area) and 15 L (membrane flux=65 $L.h^{-1}.m^{-2}$, time=12 hours and 186 cm^2 of membrane area) (Baek et al. 2011, Suwarno et al. 2012) calculated as: V(L)=Flux($L/h.m^2$)×time(h) ×Membrane Area(m^2).

Although membrane compaction is a prerequisite to most NF and RO experimental studies, including bioadhesion/biofouling, the type of water used to compact the membrane may vary considerably from one laboratory to another. The water used in recent published studies on initial adhesion and biofouling experiments spans from non-sterilised tap water (Hijnen et al. 2009, Khan et al. 2011, Vrouwenvelder et al. 2009c, Vrouwenvelder et al. 2007, Botton et al. 2012, Khan et al. 2010), DI water (Huertas et al. 2008, Herzberg and Elimelech 2007, Myint et al. 2010, Baek et al. 2011, Lee et al. 2010) and MilliQ water (Chong et al. 2008, 2007, Pang et al. 2005). Tap water and DI water will vary in quality depending on the water source and the yearly season (Gibbs et al. 1993). In essence, the total carbon, biological and endotoxin contents will differ from one water type to another, whether the water is sterilized or not. Moreover, when considering filtration aspects, all insoluble water constituents will most certainly be deposited on the membrane surface during the compaction, thus altering the membrane surface from its original state. The conditioning layer formed during the compaction pre-treatment of NF/RO is likely to result in altered surface characteristics thereby affecting subsequent biofouling experiments.

The objective of this study was to first demonstrate the impact of the choice of water used during compaction of NF membranes in terms of membrane performance, surface

121 characterisation and secondly, to investigate whether the water used during membrane
122 compaction also affects bioadhesion outcomes.

123

124 **2 Materials and Methods**

125 2.1 Water source and characterisation

126 Three different water grades were used in this study: tap water provided by south Dublin
127 water municipality, deionized water obtained by a purifying water system (Elgastat B124,
128 Veolia, Ireland) and Grade 1 pure water (18.2 $M\Omega.cm^{-1}$) obtained from an Elga Process
129 Water System (Biopure 15 and Purelab flex 2, Veolia, Ireland), hereafter referred to as
130 MilliQ water. Conductivity and pH measurements were performed on all samples at room
131 temperature (20° C) and total organic carbon of all water samples was determined using a
132 total organic carbon analyser (TOC-V_{CSH}, Shimadzu, Ireland) in the NPOC mode, equipped
133 with an automatic sample injector and an NDIR detector. Calibration standards were made
134 using potassium hydrogen phthalate at different concentrations between 0 and 10 mgC/L.
135 The water samples were collected in new 50 mL sterile Eppendorf tubes, filtered twice with
136 polyethersulphone 0.2 μm filters (Corning Incorporated, VWR Ireland), put in TOC vials that
137 had been soaked overnight in 0.5 M NaOH in MilliQ water and left to dry at 30°C upside
138 down to avoid any contamination from the air followed by a thorough rinsing with MilliQ
139 water and analysed straight away. Measurement results are presented in Table 1. The
140 measurements were carried out from samples taken between October and November 2012.
141 In the particular case of MilliQ water, the samples have a measured TOC concentration that

142 varied from 0.00 to 0.24 mgC.L^{-1}. The average value measured for 10 samples were 0.13 ±
143 0.06 mgC.L^{-1} (Table 1).

144 The total solids were measured by filling a glass vial with 40 mL of each water source and
145 allowing it to evaporate in an oven at 100°C. The vial weight was measured before and after
146 evaporation and the difference obtained in weight corresponded to the total solids weight.
147 A control sample was used, where an empty vial was placed in the oven to ensure no
148 floating particles present could affect the results.

149 The pH was measured with a HI1332 pH probe (Hannah, VWR, Ireland) and the conductivity
150 was measured with a TetraCon 325 conductivity probe (WTW, VWR, Ireland).

151 The total amount of cells in each water source was determined as follows: a volume of 100
152 mL of MilliQ and tap water and 80 ml of DI water were filtered with a 0.2 µm filter (GTBP-
153 25mm, Millipore, Ireland). The filter was then removed, placed in 3 mL of raw water without
154 carbon (as explained in section 2.3.1) and stained with SYTO® 9 and PI dyes. The filter was
155 then observed under an Epi-fluorescence microscope (Olympus BX 51) using a 40x objective.
156 Fluorescent organisms were observed using two filter cubes each exciting SYTO® 9 and PI
157 dyes at 450 nm and 550 nm respectively. At least ten micrographs were obtained at 5
158 random points on each compacted stained membrane sample. The number of fluorescent
159 organism were then counted using Image J® software (NIH, Bethesda, MD, USA).

160

161 2.2 Compaction experiment

162 NF 270 membranes (FilmTec Corp., USA) were used as the reference nanofiltration
163 membranes in this study. The membranes were gently washed and left soaking overnight in

the fridge in the water source they were going to be exposed to during the experiment in order to remove all the preservatives. The membrane compaction experiments were performed in modified Membrane Fouling Simulators (Vrouwenvelder et al. 2006) at 15 bar pressure and a feed flow rate of 0.66L.min^{-1} in each cell using one type of water grade for each experimental run. This flow rate corresponds to a velocity of 0.35 m.s^{-1}, a Re_{dh} of 579 and a shear rate of 2588 s^{-1} in each cell.

The cross-flow system was equipped with a 10 L autoclavable feed tank (Nalgene, VWR Ireland) and a high pressure pump (model P200, Hydra-Cell, UK). The system was connected to three MFS devices placed in parallel holding each NF 270 membranes on the experimental rig at the start of compaction. The MFS cells are of the slit type channel height of 0.8 mm, width of 40 mm and length of 255 mm. Each membrane cell holds a membrane of 102 cm^2. Separate experiments were carried out in the cross-flow system in order to confirm that the feed flow rate was distributed evenly by the three cells. The pressure on the outlet side of the slit feed channel of each of the 3 membrane cells was measured during operation at different flow rates and pressures. The pressure between the different MFS cells did not vary by more than 2% for the conditions tested, showing that the flow rate distributes evenly in the system. Temperature was monitored in the feed tank with a temperature indicator (model Pt 100, Radionics, Ireland) and maintained at 20ºC ± 1ºC with a coil inside the tank connected to a temperature controlled MultiTemp III water bath (Pharmacia Biotech, Ireland). A back pressure regulator (KPB1L0A415P20000, Swagelok, UK) allowed the pressurization of the system. The pressure was monitored in both feed and retentate side of the membrane cells with two pressure transducers (PTX 7500, Druck, Radionics, Ireland). The feed flow was measured using a flow meter (OG2, Nixon

Flowmeters, UK). Datalogging was set-up for monitoring inlet and outlet pressure, feed flow rate and temperature (PicoLog 1000, PicoTechnology, Radionics, Ireland). The permeate volume collected was measured using 1000 mL graduated bottles, where the permeate volume was not returned to the feed tank. The permeate flux was determined by measuring a volume of permeate with a balance HCB123 (Adams, Astech Ireland) with a stopper. The P&ID of the crossflow filtration system is depicted in Figure 1.

Permeate flux and permeate conductivity measurements were performed throughout the compaction experiment. Once permeate levels reached 0.5 L for each MFS device, the compaction was temporarily stopped to allow removal of one MFS device from the rig. Compaction was thereafter continued for the two remaining MFS devices until permeate levels reached 2 L levels each, at which point the second MFS was removed from the system. The last MFS was left compacting until 5 L permeate was collected.

Once removed from the rig system, the MFS device containing a compacted NF270 membrane was opened while submerged under the corresponding water type. Membrane samples were immediately cut to size for autopsy and dynamic adhesion experiments as described in sections 2.2.1.4 and 2.3.2. The remainder of the membrane was left to dry in a closed box at room temperature for at least 48 hours to ensure the membrane was dry.

2.2.1 Surface characterisation assays of compacted NF270 membranes.

2.2.1.1 Profilometry

Optical profilometery analysis was carried out to examine the morphology and to quantify surface roughness. These measurements were carried out using a Wyko NT1100 optical

profilometer operating in vertical scanning interferometry (VSI) mode. The R_q (root mean square roughness) was obtained on three different locations on each sample surface and an average value obtained.

2.2.1.2 Contact angle measurements

The Lifshitz-van der Waals (γ^{LW}), electron-donor (γ^-) and electron-acceptor (γ^+) surface tension components of dehydrated compacted NF 270 membrane samples (S) were determined by measuring contact angles using the following expression:

$$\cos\theta = -1 + 2\left(\gamma_S^{LW}\gamma_L^{LW}\right)^{\frac{1}{2}}/\gamma_L + 2\left(\gamma_S^{+}\gamma_L^{-}\right)^{\frac{1}{2}}/\gamma_L + 2\left(\gamma_S^{-}\gamma_L^{+}\right)^{\frac{1}{2}}/\gamma_L \quad (1)$$

Contact angles (ϑ) and surface energy measurements (γ^S) of dehydrated compacted NF 270 membrane were measured at room temperature using a goniometer (OCA 20 from Dataphysics Instruments) with three static pure liquids (L): deionised water, diiodomethane and ethylene glycol.

The Lewis acid-base component was deduced from:

$$\gamma_S^{AB} = 2\sqrt{\left(\gamma_S^{+}\gamma_S^{-}\right)} \quad (2)$$

the total surface energy was defined by:

$$\gamma_S = \gamma^{AB} + \gamma^{LW} \quad (3)$$

227 Contact angle values and determined surface energies values presented in table 2
228 represent the mean of at least 10 measurements per compacted sample membrane.
229 Contact angle measurements were repeated for two independent replicates.

230

231 ***2.2.1.3 Scanning electron microscopy***

232 For high resolution *ex-situ* observations of the membrane surface, the compacted NF 270
233 membranes were dehydrated by drying in air and then gold coated for 30 sec at x V 30 mA.
234 High magnification imaging of the membrane surfaces was performed under a Hitachi SEM
235 at the UCD Nano-imaging and Materials Analysis Centre.

236

237 ***2.2.1.4 Biological assessment of NF 270 compacted membranes***

238 For assessing the biological presence on membranes samples, three regions of the
239 compacted NF 270 membranes were cut and placed in small petri dishes containing 3mL of
240 the water grade used during compaction. Membrane samples were then stained by adding
241 0.5 µL of 3.34 mM SYTO® 9 green-fluorescent nucleic acid staining solution and 0.5 µL of 20
242 mM propidium iodide red-fluorescent nucleic stain. Stained membrane samples were
243 subsequently incubated in the dark for at least 15 minutes, after which the staining mix was
244 discarded from the petri dish and a cover slip placed on the membrane surfaces. The stained
245 sample was then observed under an Epi-fluorescence microscope (Olympus Bx 51) using a
246 20x objective. Fluorescent bacteria were observed using two filter cubes each exciting
247 SYTO® 9 and PI dyes at 450nm and 550nm respectively. Ten micrographs were obtained at 5

248 random points on each compacted stained membrane sample. The number of fluorescent
249 organism was then counted using Image J® software.

250

251 2.3 Initial adhesion assay on NF270 compacted membranes

252 **2.3.1 Microbial strain and culture conditions**

253 *Pseudomonas fluorescens* NCTC 10038 was selected for dynamic adhesion assays on the
254 compacted NF 270 membrane. The cells were stored at -20 °C with 20 % volume glycerine as
255 a cryoprotectant. Prior to experiments, cells were spread on King B agar (Oxoid) and
256 incubated at 30°C overnight. Single colonies were then inoculated and cultured at 30°C and
257 150 rpm in Raw Water (RW) medium (tryptic soy broth 0.3 $g.L^{-1}$, sodium citrate $Na_3C_6H_5O_7$
258 0.26 $g.L^{-1}$, $NaHCO_3$ 0.042 $g.L^{-1}$,NaCl 0.12 $g.L^{-1}$,KH_2PO_4 0.063 $g.L^{-1}$, $MgSO_4$ 0.15 $g.L^{-1}$, NH_4Cl
259 0.005 $g.L^{-1}$, $CaCl_2$ 0.076 $g.L^{-1}$). When cell density reached 0.270 at OD_{600}, 12 mL of the
260 overnight culture were centrifuged at 7000 rpm for 10 minutes, before discarding
261 supernatant. The remaining pellet was suspended with Raw Water medium containing no
262 carbon source (RW^{-C}) to a final volume of 1 mL. The cells were then stained by adding 0.5 µL
263 of 3.34mM SYTO® 9 and 0.5 µL of 20 mM propidium iodide, followed by a 15 minutes
264 incubation period at room temperature in the dark. The stained *Ps. fluorescens* cells were
265 then centrifuged at 7000 rpm for 10 min before discarding the supernatant. The remaining
266 pellet was re-suspended in 24 mL RW^{-C} medium prior to adhesion experiments in order to
267 attain a final cell concentration of 10^7 $cells.mL^{-1}$.

268

2.3.2 Initial adhesion assay

Initial adhesion assays were performed on freshly cut compacted membranes that were placed on a support inserted in a flow cell (Model BST FC 81 ,Biosurface Technologies Corporation, Bozeman, MT, USA) with modified channel dimensions of 0.8 by 12.7 by 47.5 mm. Compacted membranes were immobilized on the support using double sided tape, and hydration was ensured by filling the flow cell chamber with RW^{-c} prior to adhesion experiments. The flow cells allow continuous-flow and a glass viewing port for *in situ* observation using an Epi-fluorescence microscope (Olympus BX 51) with a 20x objective. After removing bubbles from the system, "zero point" images of the NF270 compacted surface were recorded using two filters with excitation wavelengths set at λ_{ex} 450 nm and λ_{ex} 550 nm respectively. The freshly stained 24 mL *Ps. fluorescens* cells suspension was then circulated in the system at a volumetric flow rate of 1.5 $ml.min^{-1}$. Adhesion was recorded 1, 5, 10, 15, 20, 25 and 30 minutes after the first observed cell adhered on the surface. Two images were recorded at λ_{ex} 450 nm and λ_{ex} 550 nm for each time-point. Images of 223 µm x 1627 µm were taken and analysed by counting adhered stained *Ps. fluorescens* cells using Image J® software.

Initial adhesion kinetics of *Ps. fluorescens* on compacted membranes was established for all water sources using the following equation:

$$q(t) = q_{\max} \times \left(1 - e^{-\beta t}\right) \quad (4)$$

where $q(t)$ is the bacterial loading as a function of time (t), the maximum cell loading q_{max}, and the accumulation factor β obtained by the exponential fit of the adhesion experimental data. The linear region of the obtained curve was used to calculate the rate of adhesion by using the following expression:

$$k_d = \frac{\theta(t)}{\Delta t} \times \frac{1}{C_0} \quad (5)$$

where, k_d is the deposition rate of *Ps. fluorescens* on NF 270 membranes, ϑ *(t)* the number of adhered cells over a time period (Δt) between two time points and C_0 the initial bacterial suspension feed concentration.

3 Results

3.1 Water quality assessment

The different water qualities used in this study for compacting NF 270 membranes were characterized prior to compaction experiments and are presented in Table 1.

No detectable solids were measured in MilliQ and deionized water samples used in this study. MilliQ water had the lowest pH, total organic carbon, and conductivity values compared to deionized and tap water, respectively. MilliQ water has a very low conductivity of 0.4 $\mu S.cm^{-1}$ followed by DI water with a conductivity of 4 $\mu S.cm^{-1}$. The highest conductivity obtained was for tap water with a value of 168 $\mu S.cm^{-1}$.

No cultivable cells (determined by CFU) were found in MilliQ water. However deionized water was found to contain 170 times the number of cultivable organisms found in tap water. Direct count analysis (counting both culturable and non-culturable cells) revealed the presence of significant higher amounts of microorganisms in all tested water samples Deionized water was found to contain 1800 and 15 times more microorganisms than in

MilliQ and tap water, respectively. Moreover, deionized water also contained 850 and 30 times the amounts of dead/injured microorganisms relative to MilliQ and tap water, respectively.

3.2 Effects of different water grades on NF 270 membrane performance during compaction.

In order to determine how each water source impacted the permeate flux during compaction, the permeate flux was measured following permeation of 0.5, 2 and 5 L water in the MFS cells. The results are presented in Figure 2. After a volume of 0.5 L of water permeated through the membrane, membranes compacted with tap water showed the lowest permeate flux of 195 $L.h^{-1}.m^{-2}$ compared to membranes compacted with deionized and MilliQ water, which had permeate fluxes of 283 and 339 $L.h^{-1}.m^{-2}$, respectively. Additionally, the use of tap water during compaction led to a constant decrease in permeate flux from 195 $L.h^{-1}.m^{-2}$ to 96 $L.h^{-1}.m^{-2}$, as permeate volume increased from 0.5 L to 5 L. Visual inspection showed that the membrane surface was light in colour at 0.5 L and gradually increased to a dark yellow colour at 5 L (not shown) for tap water. In contrast, flux stabilized following 0.5 L of permeation for membranes compacted with deionized and MilliQ water: from 2 L to 5 L the permeate flux stabilised at 251 and 301 $L.h^{-1}.m^{-2}$, respectively.

3.3. Effect of different water grades on NF 270 membrane surface properties.

The physico-chemical properties of NF 270 compacted membranes were evaluated by contact angle measurements and the associated van der Waals (γ^{LW}), Lewis Base (γ^{-}) and

334 Lewis Acid (γ^+) components are presented in Table 2. Membranes exhibited increased
335 hydrophobic character with increased permeate volumes. Membranes compacted with 5 L
336 of MilliQ water showed the lowest hydrophobic properties (ϑ_{water} =49.7), followed by
337 membranes compacted with tap water (ϑ_{water} =56), and deionized water (ϑ_{water} =68.9)
338 respectively, with the surface hydrophobicity varying in the following order: MilliQ<tap<DI
339 water. Increasing permeate volumes did not affect the van der Waals (γ^{LW}) character of the
340 compacted membranes. However, membranes compacted with deionized water showed
341 lowest van der Waal surface properties with 37 mJ. m^{-2} compared to membranes
342 compacted with MilliQ (42.3 mJ.m^{-2}) and tap (45.5 mJ.m^{-2}) water respectively. A significant
343 decrease in Lewis Base (γ^-) membrane character was noticeable from 2 L to 5 L permeation
344 using MilliQ water, whereas the same drop in Lewis base properties occurred earlier from
345 0.5 L to 2 L in membranes compacted with deionized and tap water. Membrane Lewis Acid
346 (γ+) character decreased by 2.5 fold from 0.5 L and 2 L permeated volumes of MilliQ, and
347 during 2 L to 5 L permeated volumes of deionized water. A 13.7 fold increase of Lewis Acid
348 (γ^+) character was observed in compacted membrane after permeation of 2 L to 5 L tap
349 water.

350 Roughness measurements of the different compacted membranes measured by optical
351 profilometry are also presented in Table 2. No significant differences in surface roughness
352 were observed after permeation of 0.5 L and 2 L MilliQ, deionized water, and tap water.
353 Although no differences in surface roughness were observed for membranes compacted
354 with MilliQ (511 ± 143 nm) and deionized water (562 ± 123 nm) after 5 L permeation,
355 membranes compacted with tap water showed highest roughness with values of 1166 ± 147
356 nm. Height topography results presented in Figure 3 showed that the surface of membranes

357 compacted with MilliQ water (Figure 3 A) had areas of very smooth surface topology profiles
358 and areas with irregular and heterogeneous surface topology profiles, due to what looked
359 like surface defects, presumably from the manufacturing process. Topological profiles of
360 membranes compacted with deionized (Figure 3 B) and tap water (Figure 3 C) had a
361 consistent and homogeneous roughness and no surface defects were observed. The surface
362 of NF270 membranes compacted with tap water (Figure 3 C) had however frequent high
363 narrow peaks compared to the smaller peaks obtained with the DI water compaction.

364 Closer examination of the membrane surfaces using scanning electron microscopy revealed
365 distinct levels of deposition depending on water grade (Figure 4). The virgin NF270 surface
366 was relatively smooth but with the presence of numerous large heterogeneities (Figure 4 A).
367 These structures were still visible after compaction with MilliQ water (Figure 4 B). Following
368 compaction with deionized water, the membrane's surface was covered by what seemed to
369 be a matrix layer composed of microorganisms, and biological debris and possibly organic
370 carbon (Figure 4 C). When compacted with the DI water the large heterogeneities found on
371 the virgin membrane were not present, and the fouling layer caused by the DI water
372 filtration, although rough in the nanoscale, was homogeneous in the microscale. In this case
373 a distinction needs to be made: although Table 2 shows similar roughness values (R_q) for the
374 membranes compacted with the MilliQ water and the DI water, in the first case the
375 membrane is very smooth with a scattered distribution of imperfections generally with
376 valley widths between 20 to 50 µm (Figure 3 A) and in the second case, although the
377 membrane was rough, it was homogeneously rough (Figure 3 B).

378 Membrane compaction using tap water led to significant membrane fouling, including the
379 presence of aquatic organisms such as diatoms, smaller microorganisms and a pronounced

amount of debris (*e.g.* organic carbon) (Figure 4 D). The level of membrane fouling is apparent form the degree of crack artefacts observed on the surface (Figure 4 C-D) caused by dehydration, especially in the case of samples compacted with tap water.

3.3 Biological assessment of NF 270 membranes after compaction using different water grades.

The biological characteristics of the compacted NF 270 membranes was assessed by nucleic acid BacLight® staining and is presented in Figure 5. Compaction using deionized and tap water led to a pronounced two log difference in the total presence of microorganisms (10^7 cells.cm^{-2}) on the membrane compared to membranes compacted with MilliQ water after 5L volume permeation (10^5 cells.cm^{-2}). A one log biological accumulation was noticeable from 0.5 L to 5 L permeated volumes during compaction using all tested water qualities. Compacted membranes using MilliQ water showed lowest counts of dead/injured microorganisms throughout the compaction experiment with counts below 2×10^4 cells.cm^{-2}. A significant increase in dead-injured cell counts was noticeable for membranes compacted with deionized and tap water after 5 L volume permeation.

3.4 Dynamic adhesion assay on compacted NF 270 membranes using different water grades.

Dynamic adhesion assays were performed on compacted membranes to establish whether permeation using different water qualities could affect the initial adhesion of *Ps. fluorescens* in terms of amount deposited on membranes and their deposition rates. Adhesion results

for compacted membranes which underwent 5 L permeation volumes of different water qualities are presented in Figure 6 and Table 3.

Different adhesion profiles were observed for the different compacted membranes during the 30 minutes adhesion assay. Cell adhesion was highest on membranes compacted with MilliQ water after 30 minutes with 2.6×10^{5} cells.cm^{-2} followed by cell deposition on membranes compacted with tap water at 1.0×10^{5} cells.cm^{-2} (Figure 6). Cell deposition was lowest on membranes compacted with deionized water at 0.2×10^{5} cells.cm^{-2}. The total cells adhered on the different surfaces after 30 min showed the following order: DI<tap<MilliQ water. The experimental data allowed maximum cell loadings on the different membranes to be deduced based on the kinetic model (cf. eq. 4). Membranes compacted with MilliQ water revealed the highest maximum cell loadings at 2.6×10^{5} cells×cm^{-2}, being 5 times higher than cell loadings on membranes compacted with deionized water (Table 3). No maximum could be established after 30 minutes adhesion on membranes compacted with tap water (Figure 6) since the adhesion was still in its linear phase after 30 minutes of the experiment. However, Figure 6 clearly shows that q_{max} on membranes compacted with tap water is higher than the q_{max} value obtained for membranes compacted with deionized water. Adhesion velocity was found to be slowest on membranes compacted with deionized water at 1.06×10^{-5} cm.min^{-1} and tap water at 3.13×10^{-5} cm.min^{-1}. *Ps. fluorescens* cells expressed highest adhesion velocities on membranes compacted with MilliQ water at 11.7×10^{-5} cm.min^{-1} (Table 3).

4 Discussion

The aim of this study was to investigate the effects of laboratory water quality during compaction of nanofiltration membranes in terms of performance, surface property changes as well as its influence on standard bio-adhesion assays.

Filtration performance together with the physicochemical, physical properties and biological assessment of NF270 membranes were analysed following 0.5 L, 2 L and 5 L set permeation volumes during compaction with different water sources. Dynamic bioadhesion assays were subsequently performed on the compacted NF 270 membranes using *Ps. fluorescens* cells, and experimental data was used to calculate adhesion rates as well as estimate maximum cell loadings on membranes. This allowed conclusions to be drawn about the consequential effects of laboratory water quality in membrane compaction of nanofiltration processes.

Results obtained in this study show that the water quality used during compaction of membranes, a prerequisite in most membrane research laboratories, will most certainly affect membrane surface physicochemical properties prior to performing key experiments involving bacterial adhesion. Such changes on the membrane's surface due to membrane pre-treatment might be the basis of experimental biases. Indeed, membrane compaction is in itself a form of filtration whereby the elements found in the water will end up deposited on the membrane's surface.

Membrane performance in terms of permeate flux is directly linked to water quality. The observed higher decrease in permeate flux with increased permeated volume of tap water compared to DI and MilliQ water was caused by a higher concentration in the feed solution of organic matter, ions and dissolved solids which, not only led to the formation of a thicker fouling layer on the membrane surface, but also led to a higher osmotic pressure difference

between the feed and the permeate side. In this case, a combination of the cake build-up on the membrane surface and higher ionic concentration on the feed side can aggravate the permeate flux decline due to cake enhanced concentration polarisation (Hoek and Elimelech 2003). Moreover this fouling was also visible in the form of a coloration gradient as the volume of water permeated through the membrane increased: the degree of membrane coloration (yellow coloration) increased with increasing permeation volume and decreasing water purity. A study by Van der Bruggen and Vandecasteele (2001) showed that flux decline during nanofiltration was predominantly caused by adsorption of organic compounds in aqueous solution onto the membrane, leading to the blocking of pores.

It might be surprising that the amount of microorganisms in DI water is higher compared to tap water, as DI water is purified tap water. However, the ion exchange resin has been found to be a good place for microorganisms to adhere onto and proliferate (Flemming 1987) for several reasons: (1) the negatively charged solutes such as TOC and other nutrients such as nitrate are removed from the water by the ion exchange resin and consumed by the microorganisms in the resin, (2) nutrients dissolved in tap water are used by the microorganisms in the ion exchange resin as a food source and (3) the resin itself is a possible food source for bacteria as it can leach solutes to the solution.

The deposition of solutes on the membrane surface will inevitably change the membrane surface properties. The observed change in surface hydrophobicity was dependent on the water used during compaction. The NF 270 membrane, known for its hydrophilic properties (Boussu et al. 2006), became more hydrophobic following compaction with tap and deionized water respectively. In an earlier study, Her *et al*. (2008) demonstrated that the levels of hydrophobic and hydrophilic fractions in Natural Organic Matter (NOM) in water

469 that deposited onto NF membranes determined the change in surface hydrophobicity.
470 Likewise, the observed difference in surface hydrophobicity following compaction could
471 have been attributed to the original fraction of hydrophilic levels of NOM found in the
472 tested water. Interestingly, membranes compacted with deionized water having a factor 6
473 times less total organic carbon than tap water, were found to be most hydrophobic. This
474 may suggest that the deionized water in this study might have contained a higher fraction of
475 hydrophobic NOM, most likely caused by leachable residuals from the ion exchange resin of
476 the laboratory's water purifier. Surprisingly, the biological content of the deionized water
477 was also found to be significant. The combination of high TOC and biological levels found in
478 deionized water might be an indication of a possible contaminated ion exchange resin.
479 Accordingly, simple conductivity measurements should not be the sole basis for verifying
480 the purity of deionized water. Moreover, the use of sterilized deionized water would only
481 kill the microorganisms present, but not prevent their deposition on the membrane surface
482 after compaction (Figure 7).

483 The change in surface properties following membrane compaction was sufficient to
484 influence bacterial adhesion rates. Membranes compacted with MilliQ water attained the
485 highest bioadhesion and adhesion velocities followed by membranes compacted with tap
486 water and deionized respectively. Surprisingly, the extent of cell adhesion was not
487 proportional to hydrophobicity. Despite hydrophobicity being pinpointed as one of the
488 causes for higher adhesion onto surfaces (Subramani and Hoek 2008, Myint et al. 2010, Lee
489 et al. 2010), it does not in itself explain the adhesion extent of the bacteria in this study: the
490 MilliQ water compacted membrane despite being more hydrophilic showed a higher cell
491 adhesion than the more hydrophobic surfaces of the tap and DI water compacted

membranes. This indicates that surface hydrophobicity is not the sole determining factor in cell adhesion in this study and factors other than surface hydrophobicity, such as surface topology, could play more prominent role in bioadhesion. Membranes compacted with deionized and tap water, whose surfaces were covered by a fouling layer, were showed to have an unaltered surface topology compared to MilliQ water compacted membranes. The surface heterogeneities found on membranes compacted with MilliQ water might explain the observed higher bacterial adhesion compared to the smoother and more homogenous membranes following deionized and tap water compactions. A study conducted on NF 270 membranes, linked bacterial adhesion to surface heterogeneities (Subramani and Hoek 2008). Another similar study showed that surface roughness, or more specifically surface topography capable of accommodating bacterial cells, was particularly favourable for bacterial adhesion compared to other types of surface (Medilanski et al. 2002). In general, surface roughness can create conditions for the favourable initial adhesion of a single bacterium, possibly in a topological feature and this in turn forms the seed for the subsequent growth of a micro-colony.

The roughness values obtained in this study were performed under dehydrated compacted membranes, giving rise to high roughness readings and artefacts in the form of surface cracks. However, when a specific area of 20 µm by 20 µm without cracks was analysed with the profilometer software, surface roughness was still higher for the tap water compacted membrane (425.2 nm ± 152.9) compared to the roughness obtained for DI water (164 nm ± 51.7) and MilliQ water (60.5 nm ± 17.2) compacted membranes.

The presence of microorganisms on RO/NF membranes following compaction could lead to significant degrees of bias when performing adhesion and biofouling assays. This is

515 especially important when studying biofouling using a monoculture system. The presence of
516 viable organisms on freshly compacted membrane would most certainly lead to the
517 development of unanticipated outcomes.

518

519 **5 Conclusion**

520 The impact of laboratory water quality was assessed following compaction of the NF 270
521 membrane by analysing the membrane performance and surface characteristics, as well as
522 the adhesion characteristics of *P. fluorescens*. Tap and DI water compaction resulted in a
523 cake layer on the membrane surface consisting of living and dead bacteria and diatoms,
524 organic matter, dissolved solids and other components, as these were present in the water
525 used for compaction. There was a clear difference in the performance characteristics of the
526 different membranes following compaction with different water types. Compacting with DI
527 and tap water resulted in a lower permeate flux and cell adhesion rate compared to MilliQ
528 water. In contrast, compaction with MilliQ water generated the highest fluxes through the
529 membrane and a significantly higher initial adhesion of *P. fluorescens*. The reasons for the
530 different cell adhesion rates is difficult to elucidate due to the complexity of the tap and DI
531 water. However, there seems to be a correlation with the topography of the surface: large
532 heterogeneities on the surface seem to enhance *P. fluorescens* adhesion.

533 Overall, these results illustrate the importance of laboratory water quality in the
534 compaction stage of NF/RO experiments and the consequent impact it has when
535 undertaking bacterial adhesion studies. It needs to be noted while tap and DI water quality
536 will vary significantly from laboratory to laboratory, these differences in quality can make it

difficult to compare results of adhesion studies from different research groups. The present study identifies the need for standardized protocols for studying membrane biofouling in laboratory conditions, particularly with respect to the water quality during membrane compaction procedures and for the feed solutions in subsequent experiments.

Acknowledgments

This research was supported by the European Research Council (ERC), project 278530, funded under the EU Framework Programme 7 and also with the financial support of Science Foundation Ireland under Grant Number “SFI 11/RFP.1/ENM/3145. The authors would like to thank Dr. Dennis Dowling and the Surface Engineering research group at UCD. We thank Dr. Ian Reid of the NIMAC microscopy platform UCD. We thank Mr. Pat O'Halloran for his invaluable technical assistance, and Mr. Liam Morris for the construction of the MFS devices.

References

Cyna, B., Chagneau, G., Bablon, G. and Tanghe, N. (2002) Two years of nanofiltration at the Méry-sur-Oise plant, France. Desalination 147(1–3), 69-75.

Flemming, H.C. (1997) Reverse osmosis membrane biofouling. Experimental Thermal and Fluid Science 14(4), 382-391.

Ivnitsky, H., Katz, I., Minz, D., Volvovic, G., Shimoni, E., Kesselman, E., Semiat, R. and Dosoretz, C.G. (2007) Bacterial community composition and structure of biofilms developing on nanofiltration membranes applied to wastewater treatment. Water Research 41(17), 3924-3935.

Flemming, H.C. (2002) Biofouling in water systems – cases, causes and countermeasures. Applied Microbiology and Biotechnology 59(6), 629-640.

Houari, A., Seyer, D., Couquard, F., Kecili, K., Démocrate, C., Heim, V. and Martino, P.D. (2009) Characterization of the biofouling and cleaning efficiency of nanofiltration membranes. Biofouling 26(1), 15-21.

Vrouwenvelder, H.S., van Paassen, J.A.M., Folmer, H.C., Hofman, J.A.M.H., Nederlof, M.M. and van der Kooij, D. (1998) Biofouling of membranes for drinking water production. Desalination 118(1–3), 157-166.

Vrouwenvelder, J.S., Manolarakis, S.A., van der Hoek, J.P., van Paassen, J.A.M., van der Meer, W.G.J., van Agtmaal, J.M.C., Prummel, H.D.M., Kruithof, J.C. and van Loosdrecht, M.C.M. (2008) Quantitative biofouling diagnosis in full scale nanofiltration and reverse osmosis installations. Water Research 42(19), 4856-4868.

Khan, M.T., Manes, C.-L.d.O., Aubry, C. and Croué, J.-P. (2013) Source water quality shaping different fouling scenarios in a full-scale desalination plant at the Red Sea. Water Research 47(2), 558-568.

Flemming, H.C., Schaule, G., Griebe, T., Schmitt, J. and Tamachkiarowa, A. (1997) Biofouling—the Achilles heel of membrane processes. Desalination 113(2–3), 215-225.

Hijnen, W.A.M., Castillo, C., Brouwer-Hanzens, A.H., Harmsen, D.J.H., Cornelissen, E.R. and van der Kooij, D. (2012) Quantitative assessment of the efficacy of spiral-wound membrane cleaning procedures to remove biofilms. Water Research 46(19), 6369-6381.

Vrouwenvelder, J.S., Hinrichs, C., Van der Meer, W.G.J., Van Loosdrecht, M.C.M. and Kruithof, J.C. (2009a) Pressure drop increase by biofilm accumulation in spiral wound RO and NF membrane systems: role of substrate concentration, flow velocity, substrate load and flow direction. Biofouling 25(6), 543-555.

Hijnen, W.A.M., Biraud, D., Cornelissen, E.R. and van der Kooij, D. (2009) Threshold Concentration of Easily Assimilable Organic Carbon in Feedwater for Biofouling of Spiral-Wound Membranes. Environmental Science & Technology 43(13), 4890-4895.

Ivnitsky, H., Katz, I., Minz, D., Shimoni, E., Chen, Y., Tarchitzky, J., Semiat, R. and Dosoretz, C.G. (2005) Characterization of membrane biofouling in nanofiltration processes of wastewater treatment. Desalination 185(1–3), 255-268.

Huertas, E., Herzberg, M., Oron, G. and Elimelech, M. (2008) Influence of biofouling on boron removal by nanofiltration and reverse osmosis membranes. Journal of Membrane Science 318(1–2), 264-270.

Herzberg, M. and Elimelech, M. (2007) Biofouling of reverse osmosis membranes: Role of biofilm-enhanced osmotic pressure. Journal of Membrane Science 295(1–2), 11-20.

Chong, T.H., Wong, F.S. and Fane, A.G. (2008) The effect of imposed flux on biofouling in reverse osmosis: Role of concentration polarisation and biofilm enhanced osmotic pressure phenomena. Journal of Membrane Science 325(2), 840-850.

Vrouwenvelder, J.S., Graf von der Schulenburg, D.A., Kruithof, J.C., Johns, M.L. and van Loosdrecht, M.C.M. (2009b) Biofouling of spiral-wound nanofiltration and reverse osmosis membranes: A feed spacer problem. Water Research 43(3), 583-594.
Ridgway, H.F., Rigby, M.G. and Argo, D.G. (1985) Bacterial Adhesion and Fouling of Reverse Osmosis Membranes. Journal of American Water Works Association 77(7), 97-106.
Subramani, A. and Hoek, E.M.V. (2008) Direct observation of initial microbial deposition onto reverse osmosis and nanofiltration membranes. Journal of Membrane Science 319(1–2), 111-125.
Myint, A.A., Lee, W., Mun, S., Ahn, C.H., Lee, S. and Yoon, J. (2010) Influence of membrane surface properties on the behavior of initial bacterial adhesion and biofilm development onto nanofiltration membranes. Biofouling 26(3), 313-321.
Khan, M.M.T., Stewart, P.S., Moll, D.J., Mickols, W.E., Nelson, S.E. and Camper, A.K. (2011) Characterization and effect of biofouling on polyamide reverse osmosis and nanofiltration membrane surfaces. Biofouling 27(2), 173-183.
Subramani, A., Huang, X. and Hoek, E.M.V. (2009) Direct observation of bacterial deposition onto clean and organic-fouled polyamide membranes. Journal of Colloid and Interface Science 336(1), 13-20.
Baek, Y., Yu, J., Kim, S.-H., Lee, S. and Yoon, J. (2011) Effect of surface properties of reverse osmosis membranes on biofouling occurrence under filtration conditions. Journal of Membrane Science 382(1–2), 91-99.
Fonseca, A.C., Summers, R.S., Greenberg, A.R. and Hernandez, M.T. (2007) Extra-Cellular Polysaccharides, Soluble Microbial Products, and Natural Organic Matter Impact on Nanofiltration Membranes Flux Decline. Environmental Science & Technology 41(7), 2491-2497.
Miller, D.J., Araújo, P.A., Correia, P.B., Ramsey, M.M., Kruithof, J.C., van Loosdrecht, M.C.M., Freeman, B.D., Paul, D.R., Whiteley, M. and Vrouwenvelder, J.S. (2012) Short-term adhesion and long-term biofouling testing of polydopamine and poly(ethylene glycol) surface modifications of membranes and feed spacers for biofouling control. Water Research 46(12), 3737-3753.
Bernstein, R., Belfer, S. and Freger, V. (2011) Bacterial Attachment to RO Membranes Surface-Modified by Concentration-Polarization-Enhanced Graft Polymerization. Environmental Science & Technology 45(14), 5973-5980.
Suwarno, S.R., Chen, X., Chong, T.H., Puspitasari, V.L., McDougald, D., Cohen, Y., Rice, S.A. and Fane, A.G. (2012) The impact of flux and spacers on biofilm development on reverse osmosis membranes. Journal of Membrane Science 405–406(0), 219-232.
Vrouwenvelder, J.S., van Paassen, J.A.M., van Agtmaal, J.M.C., van Loosdrecht, M.C.M. and Kruithof, J.C. (2009c) A critical flux to avoid biofouling of spiral wound nanofiltration and reverse osmosis membranes: Fact or fiction? Journal of Membrane Science 326(1), 36-44.
Vrouwenvelder, J.S., Bakker, S.M., Wessels, L.P. and van Paassen, J.A.M. (2007) The Membrane Fouling Simulator as a new tool for biofouling control of spiral-wound membranes. Desalination 204(1–3), 170-174.
Botton, S., Verliefde, A.R.D., Quach, N.T. and Cornelissen, E.R. (2012) Influence of biofouling on pharmaceuticals rejection in NF membrane filtration. Water Research (0).
Khan, M.M.T., Stewart, P.S., Moll, D.J., Mickols, W.E., Burr, M.D., Nelson, S.E. and Camper, A.K. (2010) Assessing biofouling on polyamide reverse osmosis (RO) membrane surfaces in a laboratory system. Journal of Membrane Science 349(1–2), 429-437.
Lee, W., Ahn, C.H., Hong, S., Kim, S., Lee, S., Baek, Y. and Yoon, J. (2010) Evaluation of surface properties of reverse osmosis membranes on the initial biofouling stages under no filtration condition. Journal of Membrane Science 351(1–2), 112-122.
Chong, T.H., Wong, F.S. and Fane, A.G. (2007) Enhanced concentration polarization by unstirred fouling layers in reverse osmosis: Detection by sodium chloride tracer response technique. Journal of Membrane Science 287(2), 198-210.

646 Pang, C.M., Hong, P., Guo, H. and Liu, W.-T. (2005) Biofilm Formation Characteristics of Bacterial
647 Isolates Retrieved from a Reverse Osmosis Membrane. Environmental Science & Technology 39(19),
648 7541-7550.
649 Gibbs, R.A., Scutt, J.E. and Croll, B.T. (1993) Assimilable Organic Carbon Concentrations and Bacterial
650 Numbers in a Water Distribution System. Water Science & Technology 27(3-4), 159-166.
651 Vrouwenvelder, J.S., van Paassen, J.A.M., Wessels, L.P., van Dam, A.F. and Bakker, S.M. (2006) The
652 Membrane Fouling Simulator: A practical tool for fouling prediction and control. Journal of
653 Membrane Science 281(1–2), 316-324.
654 Hoek, E.M.V. and Elimelech, M. (2003) Cake-Enhanced Concentration Polarization: A New Fouling
655 Mechanism for Salt-Rejecting Membranes. Environmental Science & Technology 37(24), 5581-5588.
656 Van der Bruggen, B. and Vandecasteele, C. (2001) Flux Decline during Nanofiltration of Organic
657 Components in Aqueous Solution. Environmental Science & Technology 35(17), 3535-3540.
658 Flemming, H.-C. (1987) Microbial growth on ion exchangers. Water Research 21(7), 745-756.
659 Boussu, K., Zhang, Y., Cocquyt, J., Van der Meeren, P., Volodin, A., Van Haesendonck, C., Martens,
660 J.A. and Van der Bruggen, B. (2006) Characterization of polymeric nanofiltration membranes for
661 systematic analysis of membrane performance. Journal of Membrane Science 278(1–2), 418-427.
662 Her, N., Amy, G., Chung, J., Yoon, J. and Yoon, Y. (2008) Characterizing dissolved organic matter and
663 evaluating associated nanofiltration membrane fouling. Chemosphere 70(3), 495-502.
664 Medilanski, E., Kaufmann, K., Wick, L.Y., Wanner, O. and Harms, H. (2002) Influence of the Surface
665 Topography of Stainless Steel on Bacterial Adhesion. Biofouling 18(3), 193-203.

666

667

668

669

670

671

672 **List of Tables**

673 Table 1 Chemical and biological characterisation of the different water qualities used during
674 the membrane compaction study**.**

675

676 Table 2 NF 270 membrane surface properties after compaction with different water sources
677 at different permeate volumes.

678

679 Table 3: Estimated maximum cell loading and adhesion velocity values of *Ps. fluorescens*
680 cells on compacted NF270 membranes with different water qualities. Error is represented as
681 standard error.

682

683

684

685 **List of Figures**

686

687 Figure 1 MFS Cross-Flow system.

688

689 Figure 2 Flux decline of the NF 270 membrane during compaction with different water
690 sources (0.5, 2 and 5 L of source water filtered, 0.66 L.min^{-1} in each MFS, 15 bar and 21°C).
691 Each experiment was repeated twice. The error bar represents the variability of the flux
692 obtained for all the membranes used in duplicate exposed to that particular permeate
693 volume (0.5, 2 and 5 L).

694

695 Figure 3 Height topography of 5L compacted membranes with MilliQ (A), DI (B) and tap
696 water(C) were obtained by optical profilometery (223 μm ×293 μm). The 2D images
697 associated to each profile are shown, all X and Y axes are in microns.

698

699 Figure 4 Scanning electron micrographs of non-compacted NF 270 virgin membranes (A) and
700 compacted NF 270 membranes after 5L permeated volumes of Milli Q water (B), deionized
701 water (C), and tap water (D) at 0.66 L.min^{-1}, 15 bar and 21°C .

702

703 Figure 5 Number of accumulated microorganisms on NF270 membranes following
704 compaction with increasing permeated volumes of different water qualities. Error bars
705 represent standard error.

706

707 Figure 6 Dynamic adhesion of *Ps. fluorescens* cells on compacted NF-270 membranes after 5
708 L permeated volumes of different water qualities.

709

710 Figure 7 Fluorescence micrographs showing membrane samples following membrane
711 compaction with autoclaved DI water at 15 bar stained with (A) Syto 9 and (B) Propidium
712 Iodide and membrane compaction with non-autoclaved DI water at 15 bar stained with (C)
713 Syto 9 and (D) Propidium Iodide

714

715

716 Table 1

Water Quality	MilliQ Water	Deionized Water	Tap Water
Total Solids ($mg.L^{-1}$)	ND*	ND*	109.17 ± 5.2
pH	6.01 ± 0.11	6.31 ± 0.29	7.44 ± 0.07
TOC ($mgC.L^{-1}$)	0.13 ± 0.06	1.6 ± 0.7	9.6 ± 0.8
Conductivity ($\mu S.cm^{-1}$)	0.4 ± 0.1	4 ± 2	168 ± 7
Culturable counts ($Cells.mL^{-1}$)	ND*	239	1.4
Total cell counts (10^3 $Cells.mL^{-1}$)	1 ± 1	1472 ± 421	123 ± 47
Total dead/injured counts (10^3 $Cells.mL^{-1}$)	3 ± 2	2020 ± 482	82 ± 44

717 *ND: not detected

718

719

720

721

Table 2

		Compacted NF 270 membranes								
		MilliQ water			Deionized water			Tap water		
	Permeated volume	0.5L	2L	5L	0.5L	2L	5L	0.5L	2L	5L
Contact angle	Θ_{water}	40.5 ± 1.11	45.5 ± 0.89	49.7 ± 0.58	55.7 ± 0.34	64.3 ± 0.45	68.9 ± 0.63	45.8 ± 0.9	53.4 ± 0.6	56.0 ± 3.9
	$\Theta_{diiodomethane}$	36.6 ± 0.41	36.9 ± 0.88	34.4 ± 0.67	45.3 ± 0.56	46.8 ± 0.88	44.6 ± 0.97	38.6 ± 0.7	36.4 ± 1.6	28.7 ± 6.7
	$\Theta_{ethylene\ glycol}$	28.9 ± 0.98	25.8 ± 0.73	26.6 ± 0.42	34.6 ± 0.64	41.5 ± 0.81	47.8 ± 0.59	32.9 ± 0.9	36.7 ± 0.7	40.6 ± 5.6
Surface tension ($mJ \cdot m^{-2}$)	γ^{LW}	41.4 ± 0.18	41.3 ± 0.41	42.3 ± 0.33	36.9 ± 0.31	35.7 ± 0.51	37.0 ± 0.56	40.3 ± 0.4	41.9 ± 0.7	45.5 ± 0.5
	γ^{-}	49.1 ± 1.83	44.8 ± 1.4	33.7 ± 0.99	28.5 ± 0.55	19.9 ± 0.85	17.8 ± 1.24	44.9 ± 1.4	35.5 ± 1.2	33.4 ± 1.2
	γ^{+}	0.1 ± 0.04	0.04 ± 0.01	0.03 ± 0.01	0.1 ± 0.02	0.2 ± 0.04	0.08 ± 0.02	0.15 ± 0.05	0.19 ± 0.04	0.55 ± 0.1
	γ^{AB}	4.06 ± 0.6	2.22 ± 0.4	1.86 ± 0.32	3.9 ± 0.4	4.9 ± 0.6	2.77 ± 0.4	3.94 ± 0.73	4.80 ± 0.8	9.1 ± 0.9
	γ^{S}	53.2 ± 2.3	47.0 ± 1.65	35.6 ± 1.03	32.5 ± 0.4	24.8 ± 0.7	20.6 ± 1.32	48.9 ± 1.9	40.3 ± 1.8	42.6 ± 2.04
Surface roughness (RMS) (nm)	200 µm x 200 µm surface area*	468 ± 142	417 ± 121	511 ± 143	452 ± 177	592 ± 144	562 ± 123	521 ± 160	695 ± 251	1166 ± 147

* Roughness deduced from surface profilometry.

Table 3

	Compacted NF 270 membranes		
	MilliQ water	Deionized water	Tap water
Estimated maximum cell loading q_{max} (10^4 Cells.cm^{-2})	26 ± 2.5	5.2 ± 1.3	ND
Adhesion velocity k_d(10^{-5} cm.min^{-1})	11.7 ± 2.4	1.06 ± 0.09	3.13 ± 0.3

*ND: not determined.

1 Figure 1

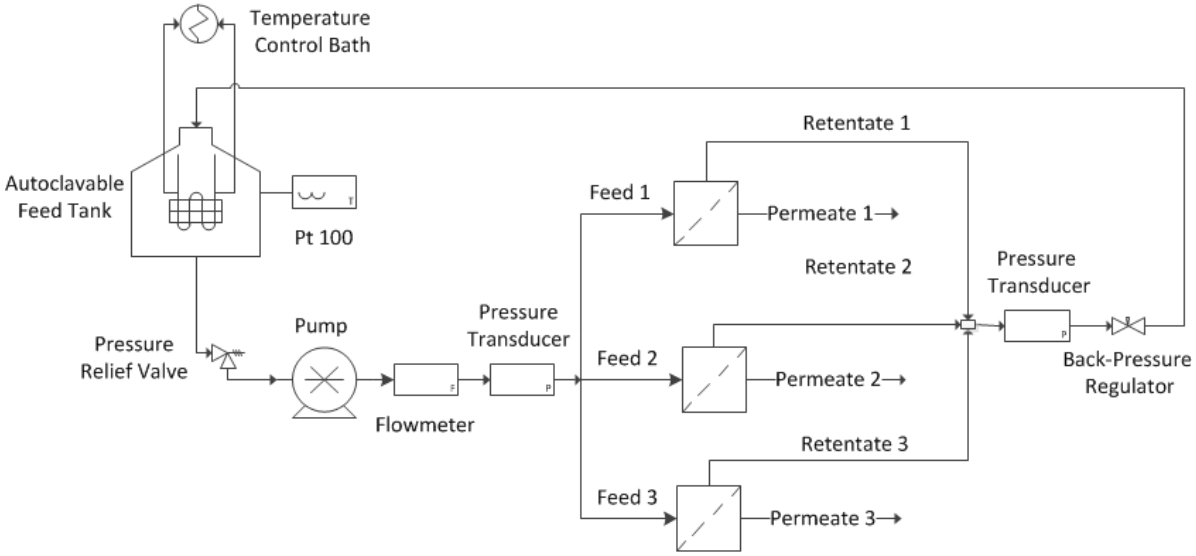
Temperature
Control Bath
Autoclavable
Feed Tank
Pt 100
Pressure
Relief Valve
Pump
Flowmeter
Pressure
Transducer
Feed 1
Feed 2
Feed 3
Retentate 1
Permeate 1
Retentate 2
Permeate 2
Retentate 3
Permeate 3
Pressure
Transducer
Back-Pressure
Regulator

2

3

1 Figure 2

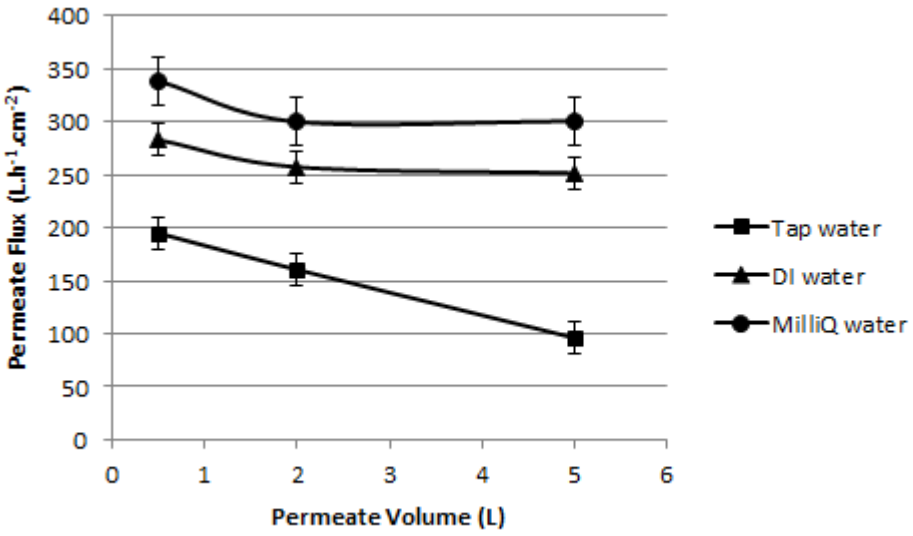
400
350
300
250
200
150
100
50
0
0
1
2
3
4
5
6
Permeate Flux (L.h-1.cm-2)
Permeate Volume (L)
Tap water
DI water
MilliQ water

2

3

Figure 3

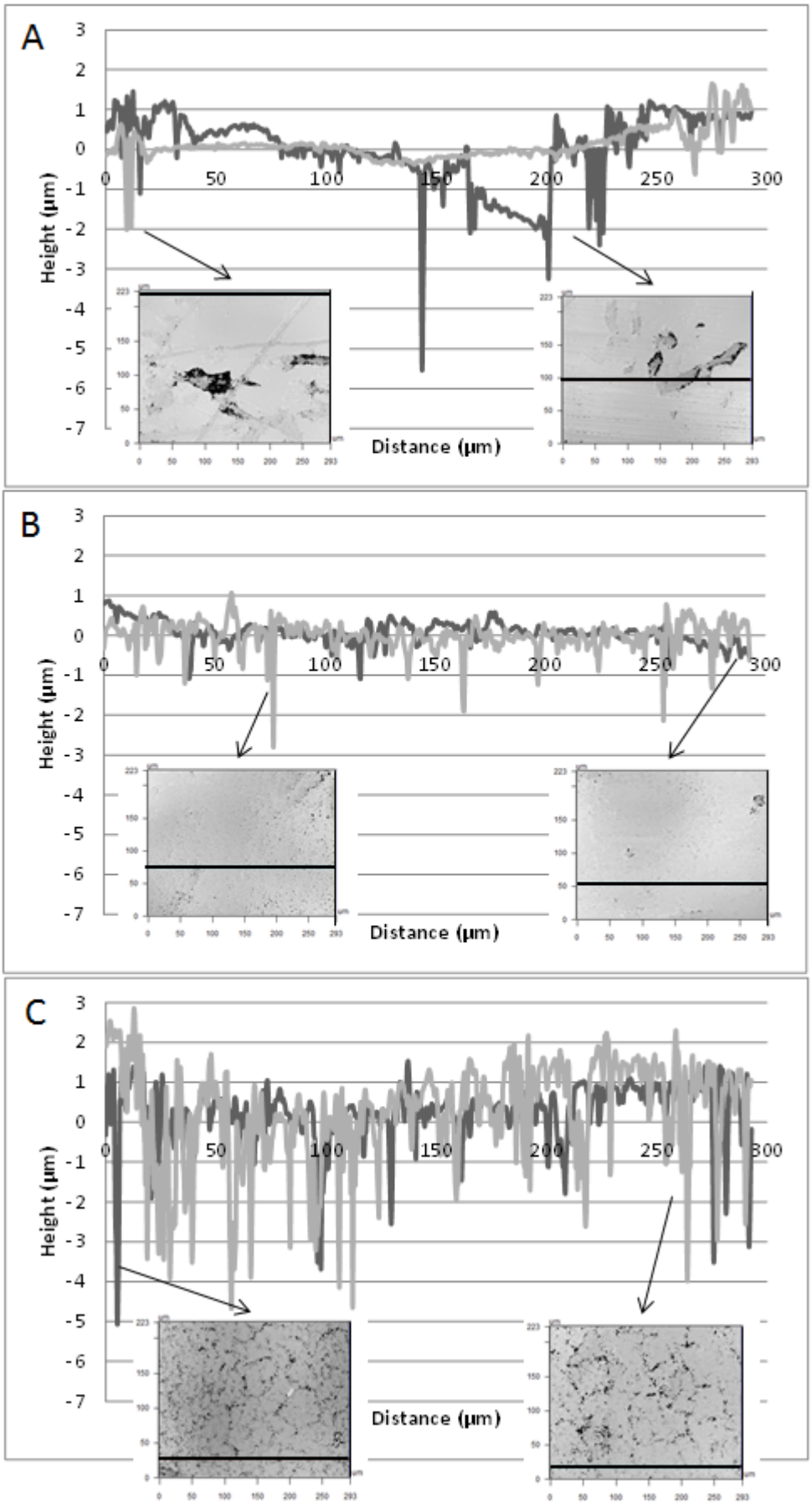
A
B
C
Height (µm)
Distance (µm)
3
2
1
0
-1
-2
-3
-4
-5
-6
-7
0
50
100
150
200
250
300

1

1 Figure 4

2 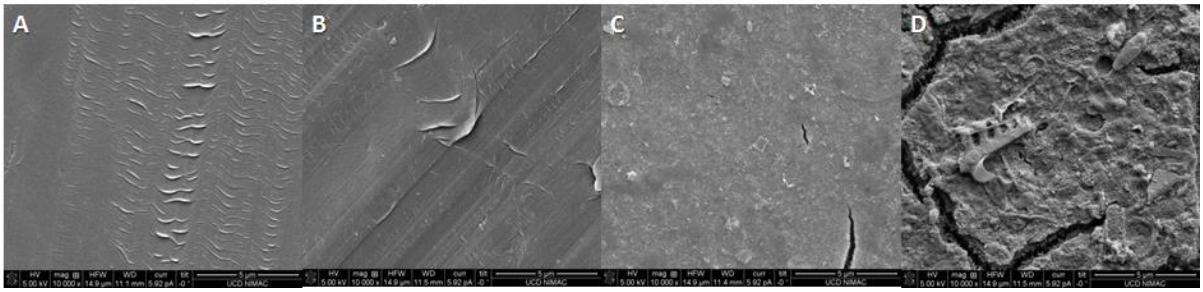

3

1 Figure 5

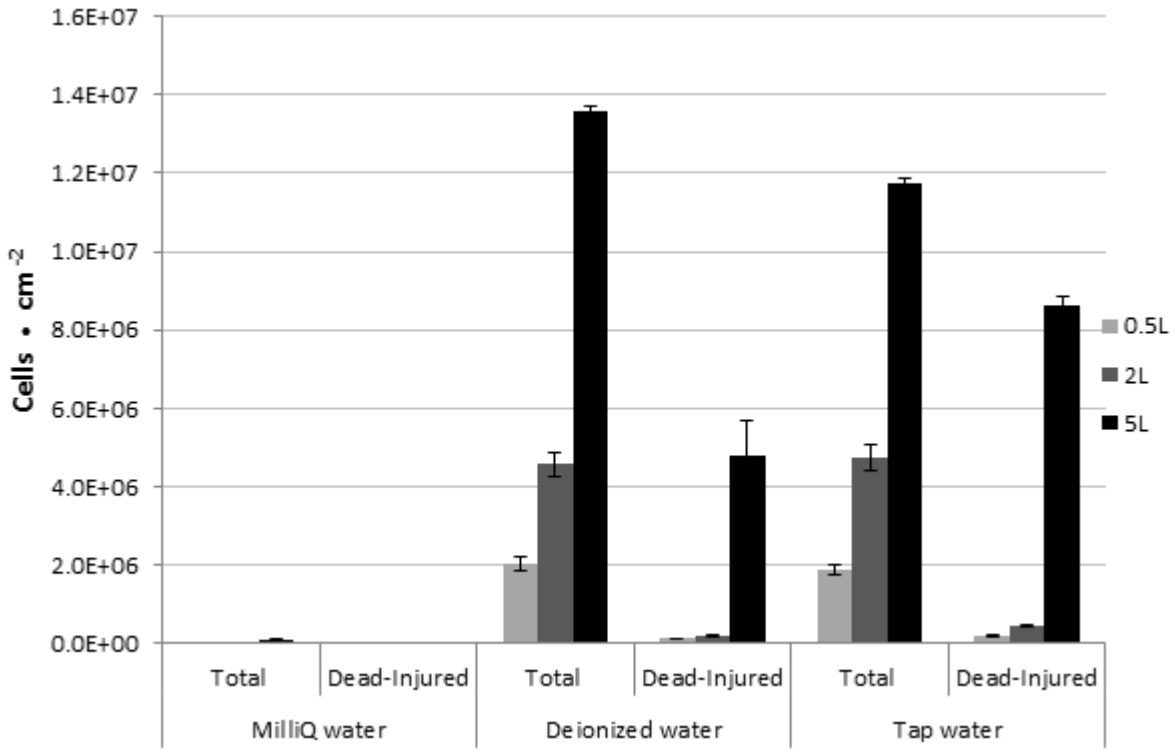
1.6E+07
1.4E+07
1.2E+07
1.0E+07
8.0E+06
6.0E+06
4.0E+06
2.0E+06
0.0E+00
Cells • cm-2
0.5L
2L
5L
Total
Dead-Injured
Total
Dead-Injured
Total
Dead-Injured
MilliQ water
Deionized water
Tap water

2

3

1 Figure 6

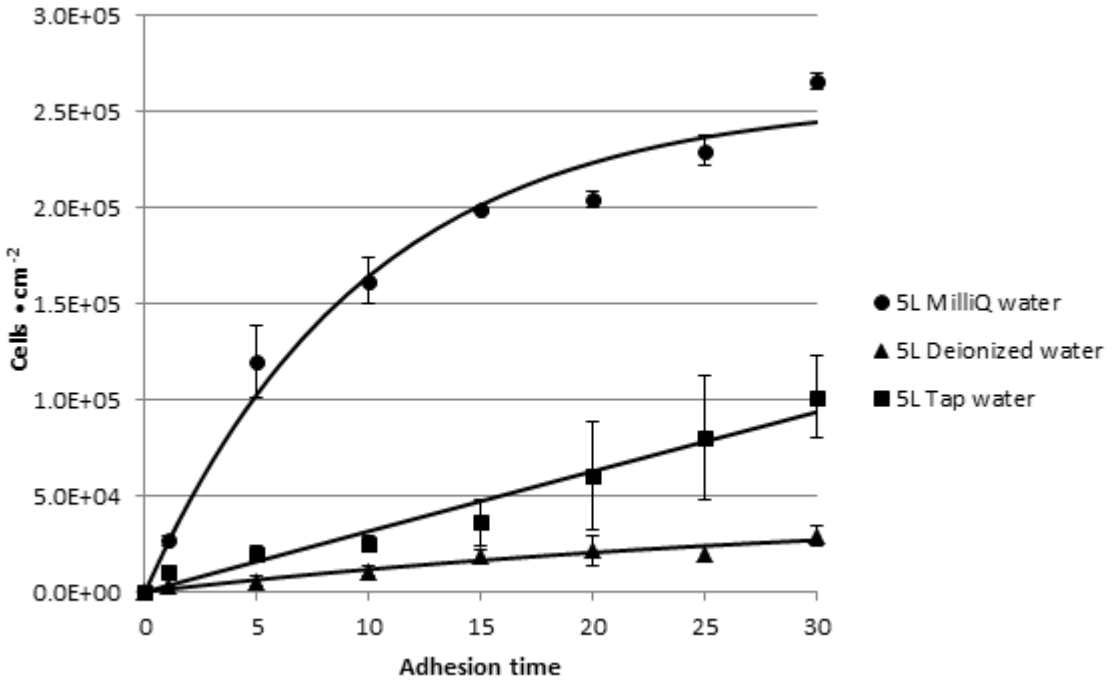
3.0E+05
2.5E+05
2.0E+05
1.5E+05
1.0E+05
5.0E+04
0.0E+00
Cells • cm-2
0
5
10
15
20
25
30
Adhesion time
5L MilliQ water
5L Deionized water
5L Tap water

2

3

Figure 7